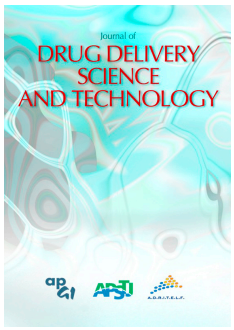

The use of new quinazolinone derivative and doxorubicin loaded solid lipid nanoparticles in reversing drug resistance in experimental cancer cell lines: A systematic study

Shahira F. El-Menshawe, Ossama M. Sayed, Heba A. Abou Taleb, Mina A. Saweris, Dana M. Zaher, Hany A. Omar

PII: S1773-2247(20)30027-7

DOI: https://doi.org/10.1016/j.jddst.2020.101569

Reference: JDDST 101569

To appear in: *Journal of Drug Delivery Science and Technology*

Received Date: 6 January 2020

Revised Date: 1 February 2020

Accepted Date: 6 February 2020

Please cite this article as: S.F. El-Menshawe, O.M. Sayed, H.A. Abou Taleb, M.A. Saweris, D.M. Zaher, H.A. Omar, The use of new quinazolinone derivative and doxorubicin loaded solid lipid nanoparticles in reversing drug resistance in experimental cancer cell lines: A systematic study, *Journal of Drug Delivery Science and Technology* (2020), doi: https://doi.org/10.1016/j.jddst.2020.101569.

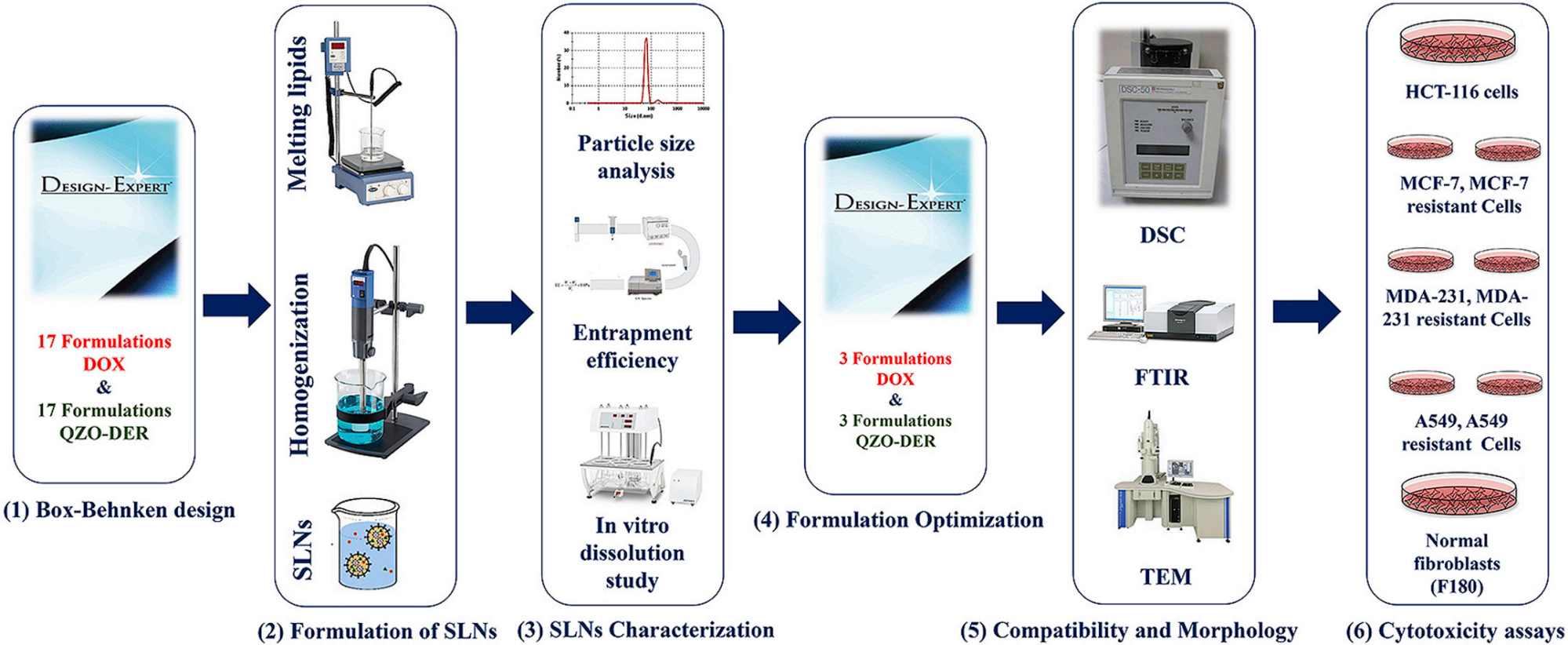
DESIGN-EXPERT
17 Formulations
DOX
&
17 Formulations
QZO-DER
(1) Box-Behnken design
Melting lipids
Homogenization
SLNs
(2) Formulation of SLNs
Particle size analysis
Entrapment efficiency
In vitro dissolution study
(3) SLNs Characterization
DESIGN-EXPERT
3 Formulations
DOX
&
3 Formulations
QZO-DER
(4) Formulation Optimization
DSC
FTIR
TEM
(5) Compatibility and Morphology
HCT-116 cells
MCF-7, MCF-7 resistant Cells
MDA-231, MDA-231 resistant Cells
A549, A549 resistant Cells
Normal fibroblasts (F180)
(6) Cytotoxicity assays

The Use of New Quinazolinone Derivative and Doxorubicin Loaded Solid Lipid Nanoparticles in Reversing Drug Resistance in Experimental Cancer Cell Lines: A Systematic Study.

Shahira F. El-Menshawe[a], Ossama M Sayed[a*], Heba A. Abou Taleb[b], Mina A. Saweris[b], Dana M. Zaher[c], Hany A. Omar[c, d*]

[a] *Department of Pharmaceutics and Industrial Pharmacy, Faculty of Pharmacy, Beni-Suef University, Beni-Suef 62514, Egypt*

[b] *Department of Pharmaceutics and Industrial Pharmacy, Faculty of Pharmacy, Nahda University, Beni-Suef, Egypt*

[c] *Sharjah Institute for Medical Research and College of Pharmacy, University of Sharjah, Sharjah 27272, United Arab Emirates*

[d] *Department of Pharmacology and Toxicology, Faculty of Pharmacy, Beni-Suef University, Beni-Suef 62514, Egypt*

***Corresponding authors:**

Ossama M Sayed, Ph.D., Department of Pharmaceutics and Industrial Pharmacy, Faculty of Pharmacy, Beni-Suef University, Beni-Suef 62514, Egypt email: usama.sayed@pharm.bsu.edu.eg

Hany A. Omar, Ph.D., Sharjah Institute for Medical Research and College of Pharmacy, University of Sharjah, Sharjah 27272, United Arab Emirates email: hanyomar@sharjah.ac.ae

Word count: Abstract: 338; Manuscript: 5256;

Ref: 74; Figures 5

Abstract:

The aim of this research is to study the feasibility of using carnauba wax as a new carrier for anticancer agents to deliver doxorubicin (DOX) as a model drug and a novel quinazolinone derivative (QZO-DER) to different types of normal and resistant cancer cell lines. A Box-Behnken design was implemented to investigate the influence of high melting point carnauba wax stabilized with cell membrane lipid (lecithin) and non-ionic biocompatible surfactant (span 60) in different concentration on particle size, entrapment efficiency of each drug and percent drug release. The solid lipid nanoparticles (SLNPs) were produced via the hot-melting homogenization technique. SLNPS particle size was from 16.58 ± 4 to 72.45 ± 1.21 nm and from 7.93 ± 1.67 to 174.31 ± 4.86 nm for DOX and QZO-DER respectively. Entrapment efficiency was from 51.78 ± 1.68% to 92.52 ± 2.47% and from 50.21 ± 1.8 to 82.95 ± 3.56% for DOX and QZO-DER respectively. While percentage of release after 36 hours was from 29.28 ± 3.89% to 78.08 ± 3.78% and from 37.5 ± 1.09 to 100 ± 1.25% for DOX and QZO-DER respectively. Selected formulations for DOX (OFX1 and OFX4) and QZO-DER (OFR4 and OFR6) were generated after validation of design. The *in vitro* anticancer activity was tested against both a panel of wild type and DOX-resistant human cancer cell lines. Cancer cell lines included colorectal cancer (HCT-116), breast cancer (MCF-7 and MDA-231), and lung adenocarcinoma (A549). Most of the tested SLNPs improved the efficacy of QZO-DER and DOX against the different cancer cell lines and have extended the spectrum to cover those accruing resistance during chemotherapy. QZO-DER loaded SLNPs exhibited highest ability to reverse the drug resistance of MDA-231 cells compared to MDA-231/ADR cells was 19.7-fold, while DOX loaded SLNPs that showed reversal power was 1.8 fold for same cells. Additionally, SLNPs showed a broad safety margin in normal cells. This study presented the use of SLNPs with carnauba wax as a potential therapeutic strategy to improve anticancer activity and overcome cancer resistance for clinical use.

Keywords: Carnauba wax; Lecithin; span 60; hot melting homogenization; resistant cancer cell lines.

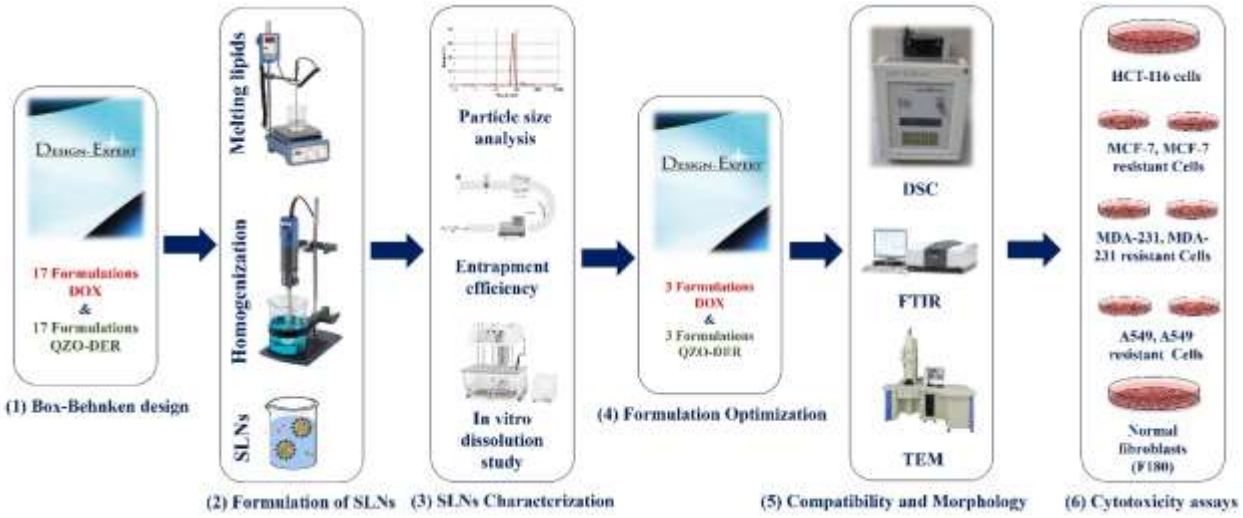

Graphical Abstract

Background:

Globally, cancer is the second major cause of mortality. In 2015, 17.5 million cases were diagnosed with cancer, which resulted in 8.7 million deaths [1]. The most four common cancer types worldwide are lung, prostate, breast, and colorectal cancer, which account for around 4 in 10 of all diagnosed cancers [2]. Therefore, cancer treatment stands at the forefront of the medical field. Cancer treatment involves a range of one or more interventions such as surgery, cryosurgery, immunotherapy, hormone therapy, radiotherapy, and chemotherapy.

However, current chemotherapeutic strategies fail to distinguish between healthy and cancerous cells, which result in a limited therapeutic effect on cancer cells, and severe adverse effects on healthy cells [3]. Since cancer cells acquire resistance to applied chemotherapeutic agents, Multidrug resistance (MDR) represents a challenge for successful treatment [4].

One of the approaches to minimize the risk of systemic toxicity, potentiate the activity of chemotherapeutic agents and overcome chemotherapeutics resistant is to design system in nano-size as nanoparticles. Nanoparticles could achieve passive targeting for tumor, which is based on the enhancement of permeability and retention effect as a result nanoparticles (NPs) might preferentially extravasate into the tumor and retain in [5].

NPs can exhibit more superior anti-cancer activity than the corresponding free drug by increasing the solubility of poorly water-soluble drugs and enhancing the drug uptake by cancer cells [6, 7].

There are various types of lipid nanoparticles that have been used to formulate anticancer agents, but more attention has been paid to solid lipid nanoparticles (SLNPs) [8]. One of the SLNPs components is the lipid matrix, which remains solid at room and body temperature compared to other lipid and polymeric nanocarriers [9]. SLNPs provide attractive features including good stability, small particle size, and controlled drug release, in addition to the

elimination of the need for toxic organic solvents [10]. Furthermore, SLNPs were identified to overcome MDR by passing through drug efflux transporters p-glycoproteins (P-gp), while protecting the embedded drugs from the external biological environment and ultimately enhancing the drug therapeutic efficacy [11]. The ability of SLNPs to overcome the P-gp role in multidrug resistance in cancer therapy was investigated. SLNPs showed an enhancement in apoptotic cell death through the increase in the cancer cell uptake of the drug [5, 12]. This improved efficacy was reported in systems utilizing several anti-cancer drugs like paclitaxel, 5-Fluorouracil, tamoxifen, anthracyclines, and others.

Carnauba wax or Brazilian wax is naturally obtained from a specific palm tree known as *Copernicia cerifera*, a plant native of the northeast of Brazil. Carnauba wax has several applications, as gelling, releasing and glazing agent. It has a high melting point (between 82.0-85.5 °C) making it a good option to be used in pharmaceutical systems, such as in the production of SLNPs [13, 14]. This type of lipid carriers has never been tested for it ability to deliver chemotherapeutic agents to cancer cells.

"2-(4-methoxyphenyl)-3-((2,3,4-trihydroxybenzylidene)amino)quinazolin-4(3H)-one" is a new Quinazolinone derivative (QZO-DER) (Figure 1) has shown to inhibit the action on phosphodiesterase (PDE4) enzyme that has been demonstrated to play a role in the angiogenesis, proliferation, and motility of multiple cancer types [15, 16]. Selective PDE4 inhibitors show antiproliferative activity against B-cells and T-cells. Based on this finding, selective PDE4 inhibitors were considered as novel anticancer agents. This was further supported by their antiproliferative effect against murine cancer cells [17].

Quinazolinone is heterocyclic compounds which contribute in a wide range of pharmaceutical interest such as anti-inflammatory [18], anticancer [19], antimicrobial [20], anticonvulsant [21], antimalarial [22], antihypertensive [23] and antileishmanial [24] and antihistaminic activity[25].

Quinazolines were the nucleus of marketed drugs as selective kinase inhibitors have the FDA approval as anti-cancer such as Gefitinib V, Erlotinib VI, and Lapatinib VII, which showed potent activity[26].

In 2013, Marwa F. Ahmed and Mahmoud Younis [19] were synthesized a novel 6,8-dibromo-4(3H)quinazolinone derivatives, these compounds were tested against breast carcinoma cell line MCF-7, where two compounds, showed extraordinary low IC_{50} = 1.7 and 1.8 µg/mL if compared to doxorubicin IC_{50} = 29.6 µg/mL. Hamdy M. Abdel-Rahman *et. al*.[27] were synthesized a novel series of quinazolin-4(3H)-one/Schiff base hybrids as phosphodiesterase 4 inhibitors. One compound (QZO-DER) showed significant antiproliferative activity with IC_{50} = 0.14, 0.08 and 0.32 µM in breast, lung, and colon cancer cell lines, respectively, compared to doxorubicin which has IC_{50} = 0.11, 3.13 and 2.75 µM, respectively in the same cancer cell lines. In addition, PDE4 inhibition has been proven to have potential chemotherapy against various types of cancer. Therefore, it is of great interest to discover ~~of~~ new selective PDE4B inhibitors with antineoplastic activity [28, 29].

Doxorubicin (DOX) (figure1), one of the anthracycline chemotherapeutic agents, has been used for more than 30 years to treat a variety of human cancers. The mechanism of its anti-cancer activity is mediated by its intercalation into DNA, inhibiting topoisomerase II, and preventing the synthesis of DNA and RNA [30]. In addition to its anti-cancer activity, DOX has short and long-term cardiac toxicity, Moreover, after an anthracyclines treatment course, many patients initially achieve a complete remission; however, approximately 70% of the patients eventually experience a disease relapse due to the development of MDR. Therefore, it is essential to develop a drug delivery system to reduce systemic toxicity and improve the anticancer activity of DOX [31, 32].

For this purpose, QZO-DER loaded SLN and DOX-loaded SLN formulations were produced to enhance the cytotoxic effect of chemotherapy by reversing the resistance of multi-drug resistant cancer cells though designing formulations that allow the drug to bypass efflux pump transport using excipient could inhibit the function of P-gp. These excipients (or additives) offer advantages of being safe, not being absorbed from the gut, pharmaceutically acceptable and have a history of being incorporated in many parenteral and enteral formulations as solubilizing or stabilizing agents.

Insert Figure (1)

Methods:

Materials

Soya lecithin (Phospholipon 90G) PhosphatidylCholine (PC) was a kind gift from Lipoid GmbH (Germany), Carnauba wax (CW) was a kind gift from Chemical Industries Development (CID) Company (Egypt), DOX was obtained from EIMC United Pharmaceuticals (Cairo, Egypt), QZO-DER was obtained as generously gift sample from Medicinal Chemistry department, Faculty of Pharmacy, Nahda University, Egypt. Span 60, Tween 80, N-butanol were purchased from Al Naser company (Egypt).

Experimental design

A three-level three-factor Box-Behnken (BB) design was employed to statistically optimize the formulation variables for preparing QZO-DER and DOX SLNPs, using Design Expert® statistical software Ver. 7.0 (Stat-Ease, Inc., MN, USA).[33] Three independent variables were evaluated: Carnauba Wax Percentage (X1), Phosphatidyl Choline Percentage (X2) and span 60 percentage (X3). The selection of lipid moiety and surfactant was based upon preliminary screening. The Particle

size (Y1: PS), Encapsulation Efficiency (Y2: EE%) and Drug release (%) (Y3: %DR) were selected as the dependent variables. The independent (low, medium and high levels) and dependent variables are shown in Table 1.

Insert Table (1)

Preparation of QZO-DER / DOX loaded SLNPs

Commercial doxorubicin was purchased as hydrochloride salt to enhance its aqueous solubility. However, for the effective incorporation of the drug in the hydrophobic SLNPs, the drug must be hydrophobized. Chemical conversion of doxorubicin-HCl into its free base (hydrophobic) was achieved through a chemical reaction with triethylamine (TEA) (0.5 ml) then doxorubicin free base was extracted by chloroform (50 ml), chloroformic extract then dried under vacuum to obtain the Crystals of DOX base [12].

SLNPs were successfully fabricated by the hot melting homogenization technique [8, 11, 34]. For this study, two matrix lipid with lipids (phospholipon 90G, CW) were chosen along with the two commonly surfactants (span 60, Tween 80) and all ingredients were carefully weighed and heated above melting point by 5 to 10 ºC up to 85 ºC. Subsequently 10 mg of either (QZO-DER or DOX) was added and dissolved completely to form a drug-lipid melt. The aqueous solution was composed of hot distilled water heated to 80 ºC then slowly added to the drug-lipid melt while stirring with maintaining the temperature to form coarse pre-emulsion. Additional homogenization was carried out by using high-speed homogenizer (IKA T-25 ULTRA-TURAX Digital Homogenizer) at 15000 rpm for 15 min to form o/w emulsion. At room temperature, the final dispersion was cooled to solidify nanoparticles forming SLNPs and the formulation was stored in tightly sealed tubes.

SLNPs characterization

Particle size analysis

The particle size was determined using photon correlation spectroscopy by Zetasizer 2000 (Malvern Instruments Ltd, Malvern, UK)[33]. The SLNPs nanosuspension was not diluted before testing and all measurements were done in triplicate using right-angle scattering at 25 ˚C.

Entrapment efficiency (EE%)

EE% has been obtained by the indirect method. The un-trapped drug was analyzed in the supernatant after cooling centrifugation (Refrigerated SIGMA 3-16K centrifuge), as previously described [33]. The concentration of QZO-DER and DOX in the aqueous phase was determined using UV–visible spectrophotometer (SHIMADZU "UV 800") at λ_{max} 342.2 and 499 respectively. Values of EE % were calculated using Eq (1).

$$EE\% = \frac{Sf - Ss}{SLN} \times 100 \qquad \text{(Eq. 1)}$$

Where Sf and Ss were the amounts of drug added in the formulation and amount of drug in the supernatant, respectively.

***In vitro* release study:**

The in vitro QZO-DER and DOX dissolution from SLNPs was performed as described before, using (ERWEKA DT 720) dissolution tester (250 ml phosphate buffer saline, 5 ml samples, temperature set to 37±0.5 ^{o}C) [35]. The samples of each formula were withdrawn from the medium and substituted with a fresh medium over a period of 36 h. The samples were then measured

spectrophotometrically at λ_{max} 304.4 for QZO-DER and λ_{max} 498 nm for DOX (SHIMADZU "UV 800")

Formulation optimization:

The optimized three formulations for each QZO-DER and DOX were obtained using the Design Expert® software by constraints on encapsulation efficiency percent of the SLNPs to obtain the highest value, on drug release to obtain the highest value and on particle size to obtain the smallest value. The recommended optimized six formulations were then prepared and evaluated in triplicate to check the validity of the calculated optimal formulation factors and predicted responses given by the software were chosen.

Transmission electron microscopy (TEM):

The particle morphology of the optimized SLNPs of QZO-DER both and DOX were examined using a transmission electron microscope JEM-1400 (JEOL Ltd., Tokyo, Japan) as stated in previous work[33].

Fourier-transform infrared spectroscopy (FTIR):

Briefly, as stated in previous work, both drugs (QZO-DER, DOX) and both optimum formulations (OFR, OFX) were all evaluated using an FTIR Spectrophotometer (Shimadzu IR-345, Japan) in an inert atmosphere over a wave number range of 4000-400 cm^{-1}[36].

Differential scanning calorimetry (DSC):

Shimadzu DSC-50 (Shimadzu Corporation, Kyoto, Japan) was used to determine the crystalline properties of different materials and Formulations[36]. The analysis was carried out at a

temperature range of 0–250°C and the heating rate was 10°C/min, at a flow rate of 25 mL/min. The DSC thermograms were recorded. The melting point and transition measurements were measured by the supplied software.

Cell viability assay

Cell line and culture conditions:

Human colorectal cancer cell line

In this study, Human colorectal cancer cell line, HCT-116 (ATCC® CCL-247™), was obtained as previously described in Saber *et al* work [37].

Human breast cancer cell lines and Human lung carcinoma

Human breast cancer cell lines (MCF-7 and MDA-231) and Human lung carcinoma (A549) were purchased from the European Collection of Cell Cultures (ECACC, UK). At Sharjah Institute for Medical Research, University of Sharjah (UAE), cells were maintained in Roswell Park Memorial Institute medium (RPMI: Sigma-Aldrich). The normal fibroblasts (F180) were kindly supplied by professor Ekkehard Dikomey (University Cancer Center, Hamburg University, Hamburg, Germany) and maintained in Dulbecco's Modified Eagle Medium (DMEM: Sigma-Aldrich).

All incubations were done with media containing 10 % fetal bovine serum (FBS) (Sigma-Aldrich) and 1 % penicillin/streptomycin (Sigma-Aldrich) at 37 ^{o}C in a humidified atmosphere of 5 % CO_2.

Generation of MCF-7, MDA-231 and A549 resistant cells to doxorubicin

MCF-7, MDA-231, and A549 cells were seeded in T75 flasks and incubated overnight at 37 ^{o}C. Then cells were treated with the IC10 of doxorubicin (Sigma-Aldrich) for each cell line. The survived population of cells was transferred to a new flask and treated with gradually increasing concentrations of doxorubicin for 8 months to develop resistance. To maintain resistance, cells were continuously treated with the IC_{10} of doxorubicin.

Human colorectal cancer cell line assay

Sulforhodamine B assay was used to evaluate cytotoxicity. Protocol conducted and interpretations was according to Vichai *et al* [38]. SLNPs and free drug were added after 24 h incubation with various concentrations and incubated at 37 °C for 48 h to determine their IC50s (the concentration of the drug required to produce 50% cell growth inhibition).

Human breast cancer cell lines and Human lung carcinoma

Cell viability was assessed using MTT assay as described above. Briefly, MCF-7, MDA-231, A549, and their generated resistant cells were seeded at 4 $\times 10^4$ cells per well in 96 well flat-bottom plates and incubated overnight. Then, cells were treated with different concentrations of doxorubicin, Standard QZO-DER, OFR4, OFR6, OFX1 and OFX4 for 48 h. The used vehicle (DMSO) was used as a negative control. After that, the media were replaced with 200 µl of media containing 0.5 mg/ml of MTT tetrazolium dye (Sigma-Aldrich, USA). Cells were incubated for 2 h at 37^{o} C. The formed formazan crystals were solubilized with 200 µl of DMSO per well. Absorbance was measured at 570 nm using a microplate reader (Thermo Scientific, UK).

Reversal power calculation

The reversal power was calculated from Eq. (2):

$$Reversal\ Power: \frac{R_f/R_N}{S_f/S_N} \qquad \text{Eq. (2)}$$

where R_f was the IC_{50} value of drug solution against drug resistant cells, R_N was the IC_{50} value of drug loaded SLN against drug resistant cells; S_f was the IC_{50} value of drug solution against drug sensitive cells, S_N was the IC_{50} value of drug loaded SLN against drug sensitive cells.

Statistical Analysis of data:

All data regarding particle size, EE%, % and %DR were analyzed by Design Expert® and differences at the $P < 0.05$ level considered significant.

Data from cell line experiments were subjected to analysis of variance (ANOVA) followed by Fisher's PSLD test for multiple comparisons among groups, and differences at the $P < 0.05$ level considered significant. All results were expressed as the mean ± SD.

Results

Effect of formulation variables on particle size

SLNPs particle size for both QZO-DER and DOX demonstrated the results in table (2). The effects of X_1, X_2, and X_3 on the SLNPs particle size (Y_1) can be illustrated through the surface response curves in figure (2). The combined effect of the X variables on Y_1 of QZO-DER showed good fitting according to the quadratic model ($p<0.05$) though logarithmic transformation according to the following equation:

$$\log P.S. = 2.11 + 0.059\,X_1 + 0.017X_2 - 0.21X_3 - 0.014X_1X_2 + 0.066X_1X_3 - 0.33X_2X_3 + 0.16X_1^2 - 0.3X_2^2 - 0.46X_3^2 \qquad \text{(Eq. 3)}$$

The combined effect of X variables on Y_1 of DOX-SLNP showed good fit according to the quadratic model ($p<0.05$) according to the following equation:

$$P.S. = 48.08 + 13.55\,X_1 + 4.46X_2 - 4.6X_3 - 2.11X_1X_2 + 16.81X_1X_3 - 8.06X_2X_3 + 5.43X_1^2 - 14.87X_2^2 - 9.5X_3^2 \quad \text{(Eq. 4)}$$

Where X_1 is the percentage of Carnauba wax, X_2 is the percentage of Phospholipids and X_3 is the concentration of span 60.

From both equations (3, 4), it was noted that increasing the percentage of both carnauba wax and PC lead to an increase in particle size, while increasing span 60 concentration lead to a significant decrease ($p<0.05$) in particle size (from 174.31 to 7.93 nm in case of QZO-DER and from 72.45 to 12.1 nm in case of DOX).

Effect of formulation variables on encapsulation efficiency percent

The entrapment efficiency (EE%) data of the formulated SLNPs are shown in table (2). The combined effect of the X_1, X_2, and X_3 on the EE% (Y_2) of the QZO-DER and DOX SLNPs can be shown through the surface response curves in figure (2). ANOVA test for the observed EE% in QZO-DER SLNPs data indicates that the quadratic model was significant and fitting for the data ($p<0.05$). The combined effect of the independent variables on EE% of QZO-DER SLNPs showed fitting according to the quadratic model according to the following equation:

$$EE\% = 73.88 + 0.052\,X_1 - 5.27\,X_2 - 0.93\,X_3 - 6.38\,X_1X_2 + 6.42\,X_1X_3 - 7.07\,X_2X_3 - 3.94\,X_1^2 - 6.32\,X_2^2 - 3.66\,X_3^2 \quad \text{(Eq. 5)}$$

The combined effect of the independent variables on EE% of DOX SLNPs showed fitting according to the quadratic model ($p<0.05$) according to the following equation:

$$EE\% = 81.6 + 0.059\,X_1 - 4.54\,X_2 - 1.53\,X_3 - 3.59\,X_1X_2 + 7.74\,X_1X_3 - 11.92\,X_2X_3 - 4.82\,X_1^2 - 7.48\,X_2^2 - 3.92\,X_3^2 \quad \text{(Eq. 6)}$$

From both equations, there was a significant positive effect ($p<0.05$) of increasing the percentage of carnauba wax on the entrapment efficiency of both drugs (from 46.42±1.78% to 76.94±2.78% for

QZO-DER and from 51.78±1.68% to 92.52±2.47% for DOX), while increasing the percentage of PC and span 60 lead to a significant decrease in EE% ($p<0.05$) [39].

Effect of formulation variables on drug release percent

Release profiles of QZO-DER and DOX from their SLNP formulations are shown in figures (3). The combined X_1, X_2 and $X_3$the %DR (Y_3) of the QZO-DER and DOX SLNPs are be shown through the surface response curves in figure (2). The combined effect of the X variables on %DR (Y_3) of QZO-DER SLNPs showed fitting ($p<0.05$) according to the quadratic model according to the following equation:

$$\%DR = 80.92 - 2.25\,X_1 + 5.6\,X_2 + 5.03\,X_3 + 2.58\,X_1X_2 + 5.3\,X_1X_3 - 0.53\,X_2X_3 + 10.29\,X_1^2 + 3.02\,X_2^2 - 4.49\,X_3^2$$

(Eq. 7)

The combined effect of X variables on Y_3 of DOX SLNPs showed fitting according to the quadratic model ($p<0.05$) according to the following equation:

$$\%DR = 63.02 - 1.53\,X_1 + 6.32\,X_2 + 5.72\,X_3 + 3\,X_1X_2 + 5.16\,X_1X_3 - 0.5\,X_2X_3 + 12\,X_1^2 + 10.5\,X_2^2 - 1.16\,X_3^2$$

(Eq. 8)

Increasing carnauba wax percentage had a negative effect of %DR and lead to slower drug release from SLNPs. These finding came in accordance with previous literature, which showed slower release with increased EE%. [40-44]. Both PC and span 60 enhanced the release of both drugs from SLNPs (78.08% and 100% for QZO-DER and DOX respectively, $p<0.05$) due to their solubilizing and surface active action [45-47].

Insert Figure (2)

Insert Table (2)

Insert Figure (3)

Release kinetics of the different SLNPs formulations of both QZO-DER and Dox are shown in table (3). Most of the formulations showed a release pattern fitting Kross-Peppas model of release with the exception of F4 and its center points (7,8,9,12) which showed more fitting in the first-order model, F1 and F14 which Fitted Hixson model and F2, F6 and F13 which fitted Higuchi model. Kross-Peppas models apply to different pharmaceutical dosage forms, where the dissolution occurs in planes which are parallel to the particle surface if the particle dimensions decreases proportionally, in such a way that the initial geometrical form keeps constant all the time [48].

Table (3) shows the expected and observed values for the optimized formulations of both DOX and QZO-DER. All observed responses didn't significantly vary from the expected values (<30% RSD) ($p>0.05$). This indicated the validity of the design for predicting optimized formulations.

Insert Table (3)

Table (4) represents the ANOVA data generated from the experimental design software regarding the significance of the effect of each variable and their interactions on the resulted responses. The table also shows the regression data represented by the values of adjusted and predicted R^2 for each variable. The table shows good linearity of the models as shown from the high levels of correlation coefficients. The high p-values of the lack of fit indicate the validity of the design.

Insert Table (4)

Release profiles of selected formulations of both QZO-DER SLNPs and DOX-SLNPs are shown in figure (3) while the release kinetics equations from fitting release data and its R^2 is shown in table (3). From the illustrated data, it was shown that half of the formulations (3 formulations) were obeying Higuchi release kinetics while the other three was following either Kross-Peppas or first order kinetics. Statistical analysis of data showed good fitting of models and reasonable precision.

Transmission electron microscopy (TEM)

Transmission electron microscope photographs of SLNPs of QZO-DER and DOX are shown in figure (4-c and d). Photographs showed spherical particles of distinct borders.

Insert Figure (4)

Differential Scanning Calorimetry (DSC)

Figure (4-a) shows the DSC thermograms of both QZO-DER, DOX, carnauba wax, phosphatidylcholine, span 60 and their physical mixtures and freeze-dried formulations. It was obvious that the melting peaks for QZO-DER and DOX at 252 and 220 ^{o}C respectively were absent in both physical mixtures and freeze-dried formulations due to their presence as amorphous states in consequence for the presence of other excipients [49-51].

Fourier transform infrared spectroscopy (FTIR)

For the IR spectrum of QZO-DER, peaks assigned to cyclic amide C=O stretch at 1635 cm^{-1} and N=C stretch of the Schiff's base, -OH stretch of phenolic characteristic peaks at 2920 and 3408 cm^{-1} were observed (figure 4-b). In the IR spectrum of DOX, the peak at 1037 and 2925 cm^{-1} confirm the presence of C-O stretch and C-C-H Aliphatic long-chain, and the peak at 3433 cm^{-1} shows –OH stretch, C=O stretch of ketone was observed at 1733 cm^{-1} (Figure 4-b). Marker peaks for DOX and QZO-DER were found in their mixtures and freeze formulations that indicate there is no interaction between drug and excipients.

Formula OFR 4, OFR 6 and OFX 4, OFX 1were selected based upon their EE%, particle size and release patterns to study their cytotoxic effect on different types and strains of cancer cell lines

Cytotoxicity assays

The anti-cancer activity of the generated solid lipid nanoparticles with their corresponding controls was evaluated using either MTT cell viability assay or SRB assay against human cancer cell lines

including MCF-7, MCF-7 resistant, MDA-231, MDA-231 resistant, A549, A549 resistant, and HCT-116 cells. Their safety was evaluated in normal cells (F180). The determined IC50 values and reversal power values are presented in table (5).

HCT-116 responded to the treatment with standard doxorubicin with IC_{50} of 10 µM. Interestingly, the treatment with OFX1 and OFX4 increased the efficacy of DOX with IC_{50} of 6.5 µM and 7 µM, respectively. In addition, OFR4 and OFR6 showed an induced anti-cancer effect with IC_{50} of 8 µM and 6.32 µM, respectively, compared to the IC_{50} of QZO-DER (28.3 µM, $p<0.05$).

In addition, Standard doxorubicin exhibited an anti-cancer effect against MCF-7 cells with IC_{50} of 1.12 µM. The developed OFX1 did not improve the Standard doxorubicin anticancer activity with IC_{50} of 1.12. Interestingly, OFX4 showed a promising potency with IC_{50} of 0.66 µM ($p<0.05$). MCF-7 cells didn't respond to the treatment with Standard QZO-DER. However, OFR4 and OFR6 improved the activity with IC_{50} of 2.9 µM and 6.12 µM respectively ($p<0.05$).

On the other hand, MCF-7 resistant cells were not responsive to Standard doxorubicin and the treatment with OFX1, and OFX4 had a considerable increase in the anti-cancer activity with IC_{50} of 2.88, 4.9 µM. Standard QZO-DER showed more potent activity in MCF-7 resistant cells compared to MCF-7 cells ($p<0.05$). Interestingly, OFR6 showed an increase in potency compared to Standard QZO-DER with IC_{50} of 1.68 µM ($p<0.05$). However, OFR4 did not have a pronounced difference with IC_{50} of 2.85 µM ($p>0.05$).

Moreover, Standard doxorubicin exhibited an anti-cancer activity against A549 cells with IC_{50} of 6.69 µM, while the developed OFR4 and OFR6 did not show promising activity ($p>0.05$). Similar to the observed response in MCF-7 cells, Standard QZO-DER had no distinct effect in A549 while OFX4 demonstrated IC_{50} of 5.9 µM. A slight increase in the effect was observed after the treatment with OFX1 ($p<0.05$).

Following the same anti-cancer activity pattern in MCF-7 resistant cells, no effect was observed for Standard doxorubicin in A549 resistant cells. However, OFX4 showed promising activity with IC_{50} of 3.5 µM. Moreover, A549 resistant cells were more sensitive to the treatment with Standard QZO-DER compared to OFR4 and OFR6 ($p<0.05$).

Furthermore, MDA-231 was not responsive to Standard doxorubicin. Interestingly, OFX1, OFX4 showed a potent anti-cancer activity with IC_{50} of 4.8, and 4.9 µM, respectively ($p<0.05$). In addition, OFR6 showed an increase in the effect with IC_{50} of 3.78 µM ($p<0.05$) compared to the Standard QZO-DER. while OFR4 did not indicate a distinct improvement in the anti-cancer activity ($p>0.05$).

In MDA-231 resistant cells, OFR4 and OFR6 improved the anti-cancer activity ($p<0.05$) of Standard QZO-DER. Interestingly, OFX1 and OFX4showed higher anti-cancer potency compared to standard doxorubicin with IC_{50} of 6.2, and 5 µM respectively ($p<0.05$).

The reversal power values of the different SLNPs of both actives showed a considerable ability of the formulations to reverse the resistance of different cell line while maintaining the safety towards the normal fibroblast lines.

The safety profiles of all tested compounds were evaluated on F180 cells. The cells viability was not affected after treatment with all compounds with IC_{50} more than 10 µM ($p>0.05$).

Insert Table (5)

Insert Figure (5)

Discussion:

SLNs are a category of remarkable drug delivery systems that have been investigated in the biomedical field for several years. One of the main explanations for the speed flourishing of SLNs

is their ability to effectively deliver both hydrophilic and hydrophobic drugs. Doxorubicin as model anti – cancer drug has a major drawback which is the development of resistance from cancer cells of different origin. The goal of this research was to study the feasibility of incorporating QZO-DER and DOX into novel lipid nanoparticles and its efficacy in eradicating different varieties of cancer cell lines. Using carnauba wax as a lipid carrier could be of great potential for further studies.

Changing the ratio of incorporated ingredients forming theses SLNPs greatly affected the particle size, EE%, and %drug release. Increasing lipid composition lead to an increase in particle size due to increased viscosity, which came in accordance with previous literature [40, 41, 43, 52-54]. On the other hand, increasing span 60 concentration did not show enough reduction in particle size until reaching a concentration of 0.2%, which was followed by a significant reduction in particle size. This could be attributed to the low HLB nature of span 60 and the combined HLB values required to emulsify carnauba wax (HLB=15) which could be achieved at the level of 0.2% span 60 combined with the fixed amount of added tween 80 [45, 47, 55]. Mixing two or more surfactants tends to stabilize the lipid dispersion and reduce the size [42, 56]. Use of PC alone as sole emulsifier may not be enough to stabilize the SLNPs owing to the difference of the HLB between PC (HLB=4) and the lipid core (HLB=15). Therefore the combination of different surfactants will lead to a stable dispersion system [42, 56].

The positive effect of increasing the concentration of carnauba wax on the EE% of both drugs came in accordance with previous literature, which indicated the compatibility of drugs with carnauba wax as lipid carrier [40, 41, 43, 52-54]. The negative effect of PC on the EE% of both drugs could be attributed to the increased permeability of the particles and increased drug solubilization and leakage of particles [45, 47, 55].

The nature of excipients considered to be a cardinal factor affecting drug release. The hydrophobic excipients used, the slower will be the drug release [57-59]. One way to change the release rate is

adding hydrophilic or hydrophobic excipients [58, 59]. Increasing carnauba wax content in the formulation lead to more slower release than low carnauba wax particles due to the hydrophobicity and high melting point of carnauba wax, which came in accordance with previous literature [60]. Such slow release will ensure the availability of the drugs within the nanoparticulate system for the delivery within cancer cells and increase the fraction of drug reaching intracellular domain through lytic effect[61]. Drug burst in some formulations may be attributed to the presence of drugs in the outer shell of the SLNPs which could happen during the formulation step where the lipid would rapidly solidify and as the drug solution becomes supersaturated upon cooling it would be concentrated in the outer shell of the SLNPs [62-64]. Other explanation is the effect of increasing the amount of phosphatidylcholine decreased the interfacial tension between the lipid moiety and the aqueous phase and lowering the melting point of the lipid moiety[65].

The complete disappearance of DOX and QZO-DER peaks in DSC thermograms might be due to the complete miscibility within the lipid components. This was previously mentioned in literature that disappearance of the melting peak is due to loss of crystallinity and increased drug thermodynamic activity[66]. These findings could augment the high entrapment efficiency into the SLNPs.

Particle size is one of the critical formulation characteristics which will alter the cellular uptake efficiency that controls the adhesive strength between nanoparticles and cellular surface[67]. Spherical particles which have a size below 200 nm tend to accumulate in tumor tissues due to increased permeability and retention [68]. Incorporating both DOX and QZO-DER in SLNPs significantly affected their behavior towards different types of cell lines. Regarding DOX, incorporation into nanocarriers greatly increased the uptake and activity against a drug-resistant cell line that could be attributed to the by-passing of the efflux P-gp system in these resistant strains.

Incorporating DOX and QZO-DER into carnauba wax lipid carriers lead to increased permeability into cancer cells either the normal or resistant types. It was well known that the incorporated tween 80 and PC as excipients in the formulation of SLNPs greatly inhibits the function of P-gp and thus offering the active inside the cells in high concentrations[69, 70]. Incorporation of phospholipids had a significant effect on the uptake and permeation of epirubicin in the work done by Yu-Li Lo [70]. These findings could be noticed from the increase of the reversal power of some of the formulations. The different tested solid lipid nanoparticles have shown a significant improvement in the anticancer activity against the resistant cells, as OFR6 in MCF-7, OFR4 in MDA-231 and OFX4 in A549 as was shown from the reversal power of each formula against the cell lines. As there are several mechanisms of cancer cells' resistance, and the most dominant mechanism is the over-expression of MDR pumps, these nanoparticles might overcome this challenge by ensuring a successful drug delivery.

Additionally, the enhanced effect could be attributed to the sustained release of the drug from the carnauba wax matrix in high concentrations within the cellular targets [71]. Our findings came in accordance with previous findings and literature [72-75]. Lipid SLN can enhance the drug transport into cancer cells by increasing cellular uptake both in sensitive and resistant cancer cells. As low intracellular drug level is the major aspect in multi-drug resistant cells when the anticancer agent was administrated, the drug concentration increase in the target cells is the key point for reversing the multi-drug resistance. Carnauba wax through its high entrapment efficiency for both actives managed to present them inside the target cells in reasonable high concentrations. Thus, the cellular drug uptake result of anticancer drug loaded SLN was consistent with its drug resistance reversal activity. In addition, SLNPs components did not show any toxic effect on the normal fibroblast F180 cell line, which indicated the safety of the lipid's compositions.

Conclusion

The present work focuses the spotlight on the potential use of carnauba wax as a novel carrier for cancer chemotherapeutic agents like the traditional doxorubicin and the novel quinazolinone derivative. The use of cell membrane lipid and surfactant resulted in significant effects on the particle size, entrapment efficiency and release percent. This research article also presented the potential use of SLNPs as an efficient carrier for anticancer drugs and revealed an interesting effect on both normal and resistant strains of different cell lines. The present study paves the way for further studies on the effectiveness of these SLNPs in in-vivo cancer animal models.

Compliance with ethical standards

Conflict of interest. The authors declare that they have no conflict of interest.

References

[1] C. Global Burden of Disease Cancer, et al., Global, Regional, and National Cancer Incidence, Mortality, Years of Life Lost, Years Lived With Disability, and Disability-Adjusted Life-years for 32 Cancer Groups, 1990 to 2015: A Systematic Analysis for the Global Burden of Disease Study, JAMA Oncology, 3 (2017) 524-548.
[2] F. Bray, et al., Global cancer transitions according to the Human Development Index (2008–2030): a population-based study, The lancet oncology, 13 (2012) 790-801.
[3] A. Banerjee, et al., Strategies for targeted drug delivery in treatment of colon cancer: current trends and future perspectives, Drug Discovery Today, 22 (2017) 1224-1232.
[4] R. Awasthi, et al., Nanoparticles in Cancer Treatment: Opportunities and Obstacles, Current drug targets, (2018).
[5] K.W. Kang, et al., Doxorubicin-loaded solid lipid nanoparticles to overcome multidrug resistance in cancer therapy, Nanomedicine: Nanotechnology, Biology and Medicine, 6 (2010) 210-213.
[6] J. Lu, et al., Mesoporous Silica Nanoparticles as a Delivery System for Hydrophobic Anticancer Drugs, Small, 3 (2007) 1341-1346.
[7] A. Jain, S.K. Jain, In vitro and cell uptake studies for targeting of ligand anchored nanoparticles for colon tumors, European Journal of Pharmaceutical Sciences, 35 (2008) 404-416.
[8] M.S. Oliveira, et al., Solid lipid nanoparticles co-loaded with doxorubicin and α-tocopherol succinate are effective against drug-resistant cancer cells in monolayer and 3-D spheroid cancer cell models, International Journal of Pharmaceutics, 512 (2016) 292-300.

[9] S. Doktorovova, et al., Nanotoxicology applied to solid lipid nanoparticles and nanostructured lipid carriers–a systematic review of in vitro data, European Journal of Pharmaceutics and Biopharmaceutics, 87 (2014) 1-18.
[10] H.M. Eid, et al., Development, Optimization, and In Vitro/In Vivo Characterization of Enhanced Lipid Nanoparticles for Ocular Delivery of Ofloxacin: the Influence of Pegylation and Chitosan Coating, AAPS PharmSciTech, 20 (2019) 183.
[11] G. Guney Eskiler, et al., Solid lipid nanoparticles: Reversal of tamoxifen resistance in breast cancer, European Journal of Pharmaceutical Sciences, 120 (2018) 73-88.
[12] R.K. Subedi, et al., Preparation and characterization of solid lipid nanoparticles loaded with doxorubicin, European Journal of Pharmaceutical Sciences, 37 (2009) 508-513.
[13] T.M. Santos, et al., Physical properties of cassava starch–carnauba wax emulsion films as affected by component proportions, International journal of food science & technology, 49 (2014) 2045-2051.
[14] A.R. Madureira, et al., Characterization of solid lipid nanoparticles produced with carnauba wax for rosmarinic acid oral delivery, RSC Advances, 5 (2015) 22665-22673.
[15] S.S. Pullamsetti, et al., Phosphodiesterase-4 promotes proliferation and angiogenesis of lung cancer by crosstalk with HIF, Oncogene, 32 (2013) 1121-1134.
[16] K. Murata, et al., Cyclic AMP specific phosphodiesterase activity and colon cancer cell motility, Clinical & Experimental Metastasis, 18 (2000) 599-604.
[17] L. Hirsh, et al., Phosphodiesterase inhibitors as anti-cancer drugs, Biochemical Pharmacology, 68 (2004) 981-988.
[18] S.E. Abbas, et al., New quinazolinone-pyrimidine hybrids: synthesis, anti-inflammatory, and ulcerogenicity studies, European Journal of Medicinal Chemistry, 53 (2012) 141-149.
[19] M.F. Ahmed, M. Youns, Synthesis and biological evaluation of a novel series of 6,8-dibromo-4(3H)quinazolinone derivatives as anticancer agents, Archiv der Pharmazie, 346 (2013) 610-617.
[20] M.A. El-Hashash, et al., Synthesis, Antimicrobial and Anti-inflammatory Activity of Some New Benzoxazinone and Quinazolinone Candidates, Chemical and Pharmaceutical Bulletin, 64 (2016) 263-271.
[21] M.M. Aly, et al., Synthesis of some new 4(3H)-quinazolinone-2-carboxaldehyde thiosemicarbazones and their metal complexes and a study on their anticonvulsant, analgesic, cytotoxic and antimicrobial activities - part-1, European Journal of Medicinal Chemistry, 45 (2010) 3365-3373.
[22] S. Zhu, et al., Synthesis and evaluation of 4-quinazolinone compounds as potential antimalarial agents, European Journal of Medicinal Chemistry, 45 (2010) 3864-3869.
[23] V. Alagarsamy, U.S. Pathak, Synthesis and antihypertensive activity of novel 3-benzyl-2-substituted-3H-[1,2,4]triazolo[5,1-b]quinazolin-9-ones, Bioorg Med Chem, 15 (2007) 3457-3462.
[24] Y.S. Birhan, et al., Synthesis and antileishmanial evaluation of some 2,3-disubstituted-4(3H)-quinazolinone derivatives, Organic and Medicinal Chemistry Letters, 4 (2014) 10.
[25] M. Gobinath, et al., Design, synthesis and H1-antihistaminic activity of novel 1-substituted-4-(3-chlorophenyl)-[1,2,4] triazolo [4,3-a] quinazolin-5(4H)-ones, Journal of Saudi Chemical Society, 19 (2015) 282-286.
[26] W.W. Li, et al., Taking quinazoline as a general support-Nog to design potent and selective kinase inhibitors: application to FMS-like tyrosine kinase 3, ChemMedChem, 5 (2010) 513-516.
[27] H.M. Abdel-Rahman, et al., Novel quinazolin-4(3H)-one/Schiff base hybrids as antiproliferative and phosphodiesterase 4 inhibitors: design, synthesis, and docking studies, Archiv der Pharmazie, 347 (2014) 650-657.

[28] P.J. Barnes, New anti-inflammatory targets for chronic obstructive pulmonary disease, Nature Reviews Drug Discovery, 12 (2013) 543-559.
[29] J.M. Michalski, et al., PDE4: a novel target in the treatment of chronic obstructive pulmonary disease, Clinical Pharmacology & Therapeutics, 91 (2012) 134-142.
[30] O. Tacar, et al., Doxorubicin: an update on anticancer molecular action, toxicity and novel drug delivery systems, Journal of Pharmacy Pharmacology, 65 (2013) 157-170.
[31] J. Pan, et al., Polymeric Co-Delivery Systems in Cancer Treatment: An Overview on Component Drugs' Dosage Ratio Effect, Molecules, 24 (2019) 1035.
[32] C. Sun, et al., Improved antitumor activity and reduced myocardial toxicity of doxorubicin encapsulated in MPEG-PCL nanoparticles, Oncology reports, 35 (2016) 3600-3606.
[33] H.F. Salem, et al., Formulation design and optimization of novel soft glycerosomes for enhanced topical delivery of celecoxib and cupferron by Box-Behnken statistical design, Drug Development and Industrial Pharmacy, 44 (2018) 1871-1884.
[34] A. Dingler, S. Gohla, Production of solid lipid nanoparticles (SLN): scaling up feasibilities, Journal of Microencapsulation, 19 (2002) 11-16.
[35] G. Fetih, et al., Liposomal gels for site-specific, sustained delivery of celecoxib: in vitro and in vivo evaluation, Drug Development Research, 75 (2014) 257-266.
[36] V. Venkateswarlu, K. Manjunath, Preparation, characterization and in vitro release kinetics of clozapine solid lipid nanoparticles, Journal of Controlled Release, 95 (2004) 627-638.
[37] M.M. Saber, et al., Targeting colorectal cancer cell metabolism through development of cisplatin and metformin nano-cubosomes, BMC Cancer, 18 (2018) 822.
[38] V. Vichai, K.J.N.p. Kirtikara, Sulforhodamine B colorimetric assay for cytotoxicity screening, Nature Protocols 1 (2006) 1112.
[39] H.M. Aboud, et al., Nanotransfersomes of carvedilol for intranasal delivery: formulation, characterization and in vivo evaluation, Drug Delivery, 23 (2016) 2471-2481.
[40] L. Becker Peres, et al., Solid lipid nanoparticles for encapsulation of hydrophilic drugs by an organic solvent free double emulsion technique, Colloids Surf B Biointerfaces, 140 (2016) 317-323.
[41] L.I. Giannola, et al., Carnauba Wax Microspheres Loaded with Valproic Acid: Preparation and Evaluation of Drug Release, Drug Development and Industrial Pharmacy, 21 (2008) 1563-1572.
[42] S. Kheradmandnia, et al., Preparation and characterization of ketoprofen-loaded solid lipid nanoparticles made from beeswax and carnauba wax, Nanomedicine, 6 (2010) 753-759.
[43] S. Xie, et al., Preparation, characterization and pharmacokinetics of enrofloxacin-loaded solid lipid nanoparticles: influences of fatty acids, Colloids Surf B Biointerfaces, 83 (2011) 382-387.
[44] Y. Miyagawa, et al., Controlled-release of diclofenac sodium from wax matrix granule, International Journal of Pharmaceutics, 138 (1996) 215-224.
[45] C.D. Pizzol, et al., Influence of surfactant and lipid type on the physicochemical properties and biocompatibility of solid lipid nanoparticles, International Journal of Environmental Research and Public Health, 11 (2014) 8581-8596.
[46] R. Jalil, J.R. Nixon, Microencapsulation using poly (L-lactic acid) II: Preparative variables affecting microcapsule properties, Journal of Microencapsulation, 7 (1990) 25-39.
[47] M.A. Schubert, C.C. Muller-Goymann, Characterisation of surface-modified solid lipid nanoparticles (SLN): influence of lecithin and nonionic emulsifier, European Journal of Pharmaceutics and Biopharmaceutics, 61 (2005) 77-86.
[48] S. Chen, et al., Preparation and in vitro evaluation of a novel combined multiparticulate delayed-onset sustained-release formulation of diltiazem hydrochloride, Pharmazie, 62 (2007) 907-913.

[49] R. Cavalli, et al., Study by X-Ray powder diffraction and differential scanning calorimetry of two model drugs, phenothiazine and nifedipine, incorporated into lipid nnoparticles, European Journal of Pharmaceutical Sciences, 41 (1995) 329-335.
[50] R. Cavalli, Sterilization and freeze-drying of drug-free and drug-loaded solid lipid nanoparticles, International Journal of Pharmaceutics, 148 (1997) 47-54.
[51] S.C. Yang, J.B. Zhu, Preparation and characterization of camptothecin solid lipid nanoparticles, Drug Development and Industrial Pharmacy, 28 (2002) 265-274.
[52] P. Caron, T. Khan, Evolution of Ni-based superalloys for single crystal gas turbine blade applications, Aerospace Science and Technology, 3 (1999) 513-523.
[53] S. Kheradmandnia, et al., Preparation and characterization of ketoprofen-loaded solid lipid nanoparticles made from beeswax and carnauba wax, Nanomedicine, 6 (2010) 753-759.
[54] J.R. Villalobos-Hernandez, C.C. Muller-Goymann, Novel nanoparticulate carrier system based on carnauba wax and decyl oleate for the dispersion of inorganic sunscreens in aqueous media, European Journal of Pharmaceutics and Biopharmaceutics, 60 (2005) 113-122.
[55] S. Khoee, M. Yaghoobian, An investigation into the role of surfactants in controlling particle size of polymeric nanocapsules containing penicillin-G in double emulsion, European Journal of Medicinal Chemistry, 44 (2009) 2392-2399.
[56] C.-C. Chen, et al., Effects of lipophilic emulsifiers on the oral administration of lovastatin from nanostructured lipid carriers: physicochemical characterization and pharmacokinetics, European Journal of Pharmaceutics and Biopharmaceutics, 74 (2010) 474-482.
[57] Y. Akiyama, et al., Novel oral controlled-release microspheres using polyglycerol esters of fatty acids, Journal of Controlled Release, 26 (1993) 1-10.
[58] M.D. Del Curto, et al., Lipid microparticles as sustained release system for a GnRH antagonist (Antide), Journal of Controlled Release, 89 (2003) 297-310.
[59] M. Savolainen, et al., Evaluation of controlled-release polar lipid microparticles, International Journal of Pharmaceutics, 244 (2002) 151-161.
[60] H.M. Eid, et al., Development, Optimization, and In Vitro/In Vivo Characterization of Enhanced Lipid Nanoparticles for Ocular Delivery of Ofloxacin: the Influence of Pegylation and Chitosan Coating, AAPS PharmSciTech , 20 (2019) 183.
[61] J.O. Kim, et al., Cross-linked polymeric micelles based on block ionomer complexes, Mendeleev Communications, 23 (2013) 179-186.
[62] A.A. Date, et al., Parasitic diseases: liposomes and polymeric nanoparticles versus lipid nanoparticles, Advanced drug delivery reviews, 59 (2007) 505-521.
[63] S. Bose, et al., Formulation optimization and topical delivery of quercetin from solid lipid based nanosystems, International Journal of Pharmaceutics, 441 (2013) 56-66.
[64] A. Jain, et al., Mannosylated solid lipid nanoparticles as vectors for site-specific delivery of an anti-cancer drug, Journal of Controlled Release,148 (2010) 359-367.
[65] S. Benita, et al., 5-Fluorouracil: carnauba wax microspheres for chemoembolization: an in vitro evaluation, Journal of Pharmaceutical Sciences, 75 (1986) 847-851.
[66] H.M. Aboud, et al., Development, Optimization, and Evaluation of Carvedilol-Loaded Solid Lipid Nanoparticles for Intranasal Drug Delivery, AAPS PharmSciTech, 17 (2016) 1353-1365.
[67] D.R. Elias, et al., Effect of ligand density, receptor density, and nanoparticle size on cell targeting, Nanomedicine, 9 (2013) 194-201.
[68] S. Li, et al., An arginine derivative contained nanostructure lipid carriers with pH-sensitive membranolytic capability for lysosomolytic anti-cancer drug delivery, International Journal of Pharmaceutics, 436 (2012) 248-257.

[69] T.R. Buggins, et al., The effects of pharmaceutical excipients on drug disposition, Advanced Drug Delivery Reviews,59 (2007) 1482-1503.
[70] Y.-L. Lo, Phospholipids as multidrug resistance modulators of the transport of epirubicin in human intestinal epithelial Caco-2 cell layers and everted gut sacs of rats, Biochemical Pharmacology, 60 (2000) 1381-1390.
[71] G. Di Bernardo, et al., Impact of histone deacetylase inhibitors SAHA and MS- 275 on DNA repair pathways in human mesenchymal stem cells, Journal of Cellular Physiology, 225 (2010) 537-544.
[72] H. Meng, et al., Engineered design of mesoporous silica nanoparticles to deliver doxorubicin and P-glycoprotein siRNA to overcome drug resistance in a cancer cell line, ACS Nano, 4 (2010) 4539-4550.
[73] C.E. Soma, et al., Reversion of multidrug resistance by co-encapsulation of doxorubicin and cyclosporin A in polyalkylcyanoacrylate nanoparticles, Biomaterials, 21 (2000) 1-7.
[74] M.J. Shieh, et al., Reversal of doxorubicin-resistance by multifunctional nanoparticles in MCF-7/ADR cells, Journal of Controlled Release, 152 (2011) 418-425.
[75] H.L. Wong, et al., A mechanistic study of enhanced doxorubicin uptake and retention in multidrug resistant breast cancer cells using a polymer-lipid hybrid nanoparticle system, The Journal of pharmacology and experimental therapeutics, 317 (2006) 1372-1381.

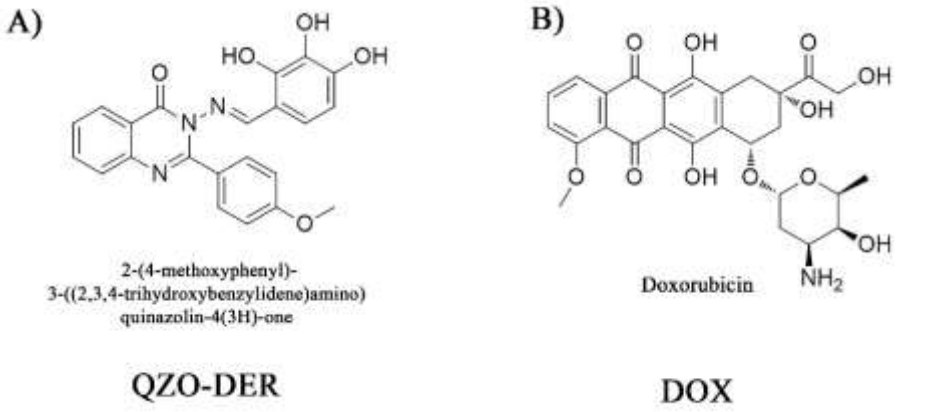

Figure (1)

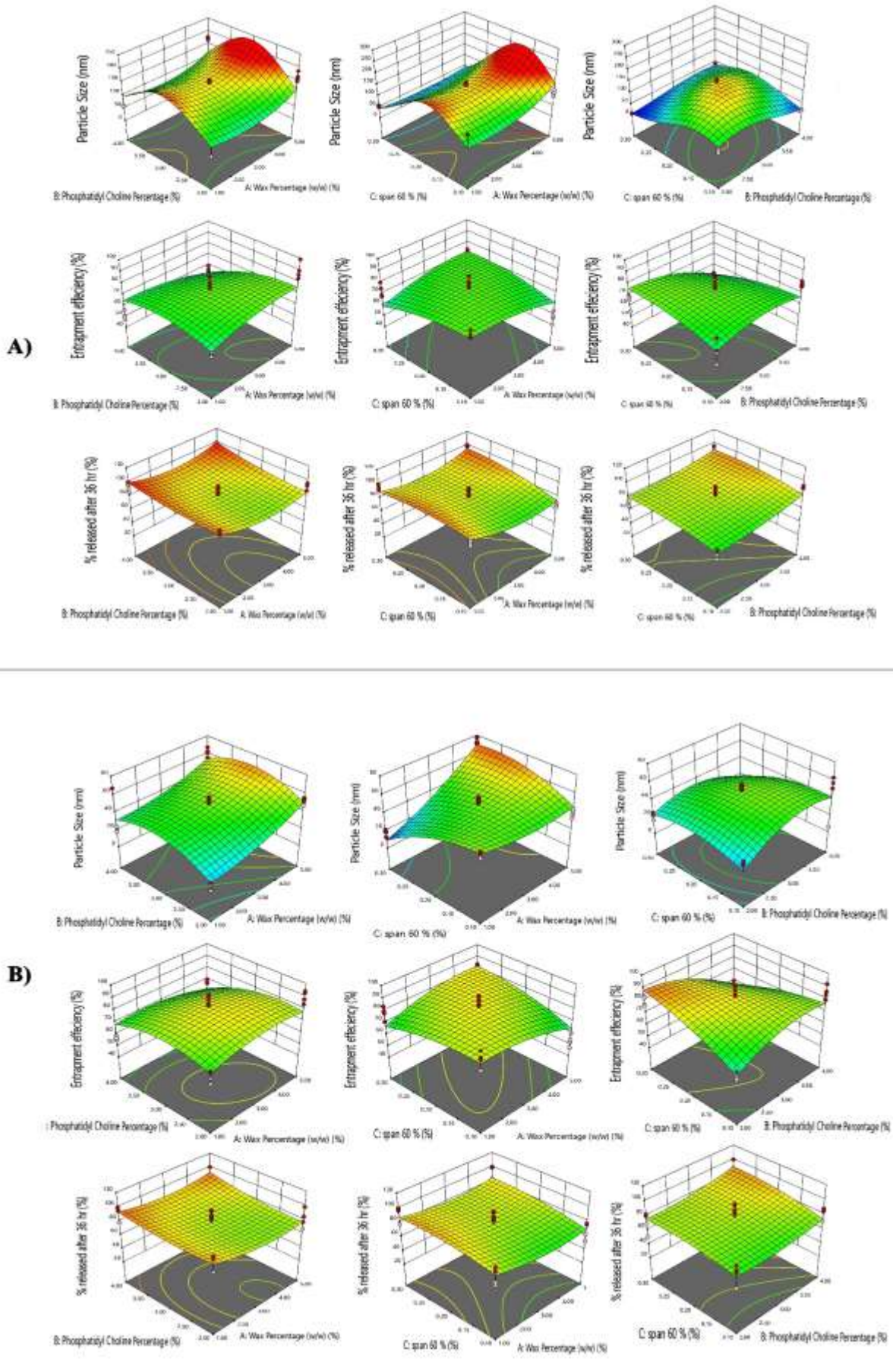
A)
Particle Size (nm)
Entrapment efficiency (%)
% released after 36 hr (%)
B: Phosphatidyl Choline Percentage (%)
A: Wax Percentage (w/w) (%)
C: span 60 % (%)
B)

Figure (2)

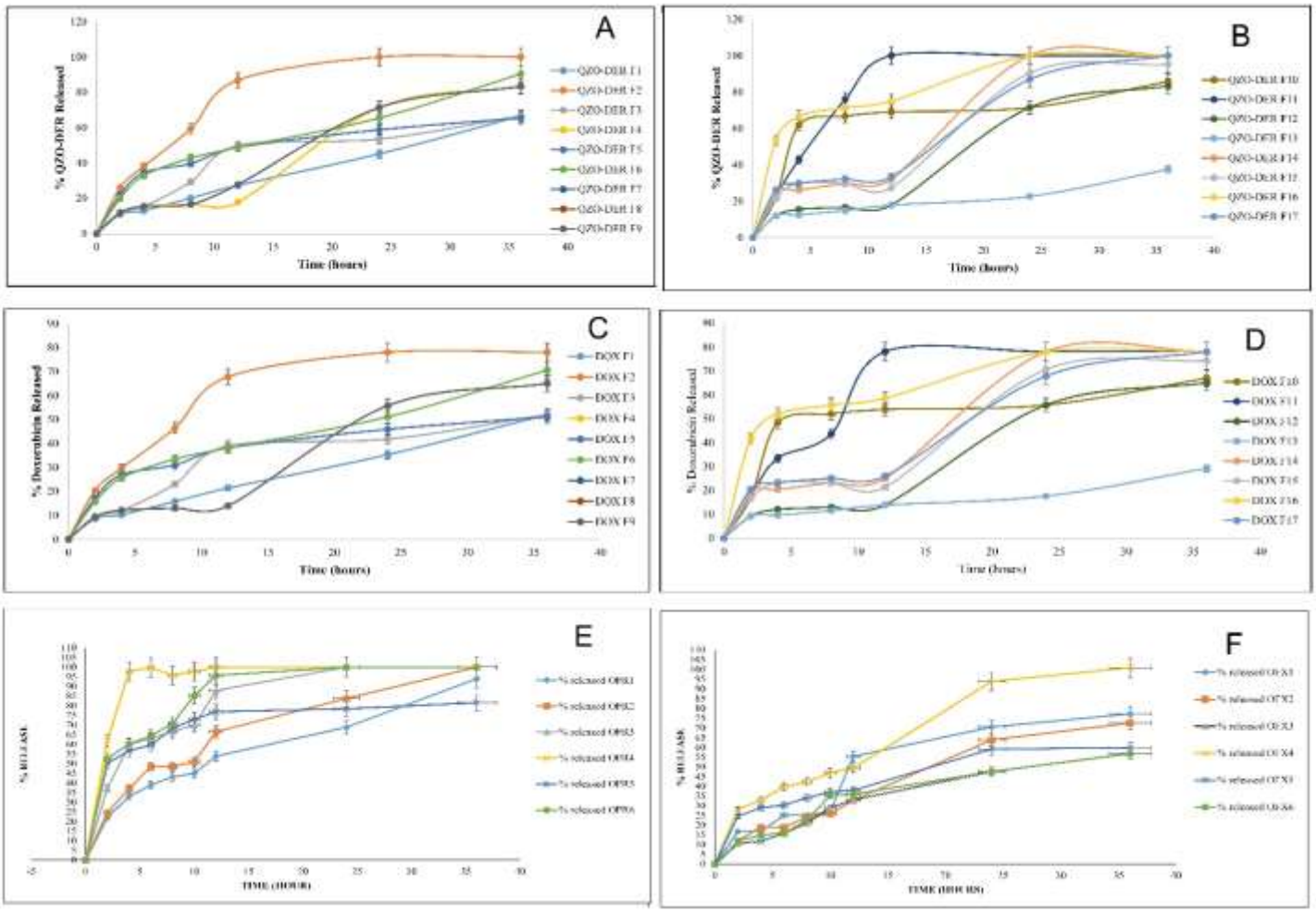
A
% QZO-DER Released
Time (hours)
B
% QZO-DER Released
Time (hours)
C
% Doxorubicin Released
Time (hours)
D
% Doxorubicin Released
Time (hours)
E
TIME (HOUR)
F
TIME (HOUR HS)

Figure (3)

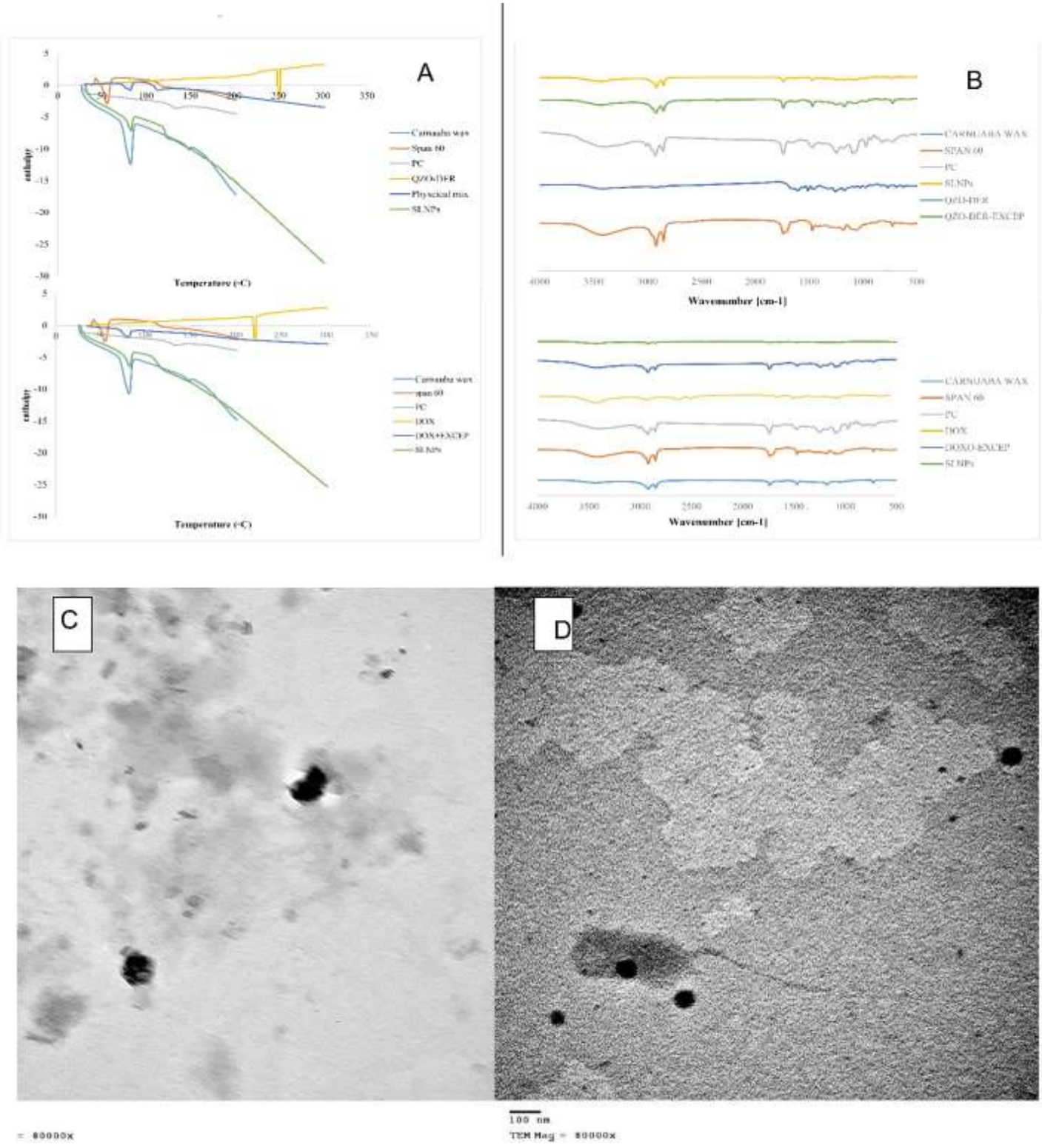
A
Temperature (°C)
Temperature (°C)
B
Wavenumber (cm-1)
Wavenumber (cm-1)
C
D
100 nm
TEM Mag = 80000x

Figure (4)

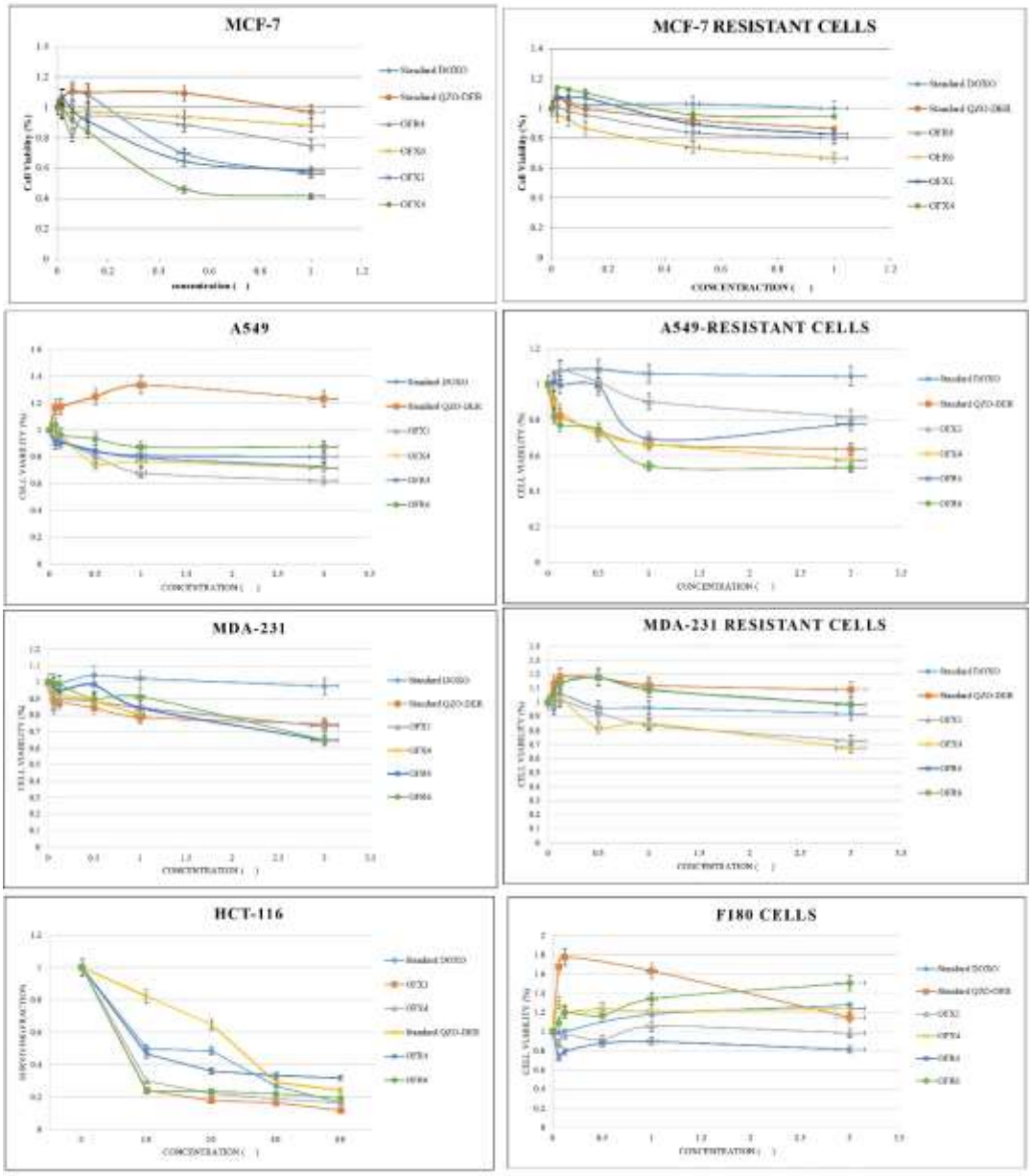
MCF-7
MCF-7 RESISTANT CELLS
A549
A549-RESISTANT CELLS
MDA-231
MDA-231 RESISTANT CELLS
HCT-116
FI80 CELLS

Figure (5)

Figure legends

Figure (1): Chemical Structure of (a) QZO-DER and (b) doxorubicin.

Figure (2): Surface response curves of the combined effect of the two independent variables on the particle size, EE% and % drug released of (a) QZO-DER and (b) DOX SLNPs SLNPs at the middle level of the third variable

Figure (3): Release profiles of QZO-DER and Doxorubicin from design (a-d) and optimized (e,f) SLNPs formulations

Figure (4): A) DSC thermograms of QZO-DER and DOX as pure state, in physical mixtures and in freeze-dried final formulations **B**) FT-IR spectra of QZO-DER and DOX as pure state, in physical mixtures and in freeze-dried final formulations. TEM photographs of **C)** QZO-DER and **D)** DOX SLNPs

Figure (5): Cytotoxicity evaluation using either MTT cell viability assay or SRB assay against human cancer cell lines including MCF-7, MCF-7 resistant, MDA-231, MDA-231 resistant, A549, A549 resistant, F180 and HCT-116 cells.

Table (1): Box-Behnken design (BBD) for optimization and composition of the QZO-DER and DOX SLNPs

Factors (independent variables)	Levels		
	Low (-1)	**Medium (0)**	**High (+)**
X_1: Carnauba Wax Percentage (w/w)	1	3	5
X_2: Phosphatidyl Choline Percentage (w/w)	2	3	4
X_3: span 60 percentage (w/w)	0.1	0.2	0.3
Responses (dependent variables)	**Constraints**		
Y_1: Particle size (nm)	Minimize		
Y_2: Encapsulation Efficiency (%)	Maximize		
Y_3: Drug release (%)	Maximize		

Run		Factors levels in actual values		
		X_1 (Carnauba wax %)	**X_2 (PC %)**	**X_3 (Span 60 %)**
Midpoints				
QZO-DER F1	**DOX F1**	3	2	0.1
QZO-DER F2	**DOX F2**	1	4	0.2
QZO-DER F3	**DOX F3**	5	3	0.1
QZO-DER F5	**DOX F5**	3	2	0.3
QZO-DER F6	**DOX F6**	3	4	0.1
QZO-DER F10	**DOX F10**	5	2	0.2
QZO-DER F11	**DOX F11**	1	3	0.3
QZO-DER F13	**DOX F13**	1	3	0.1
QZO-DER F14	**DOX F14**	5	4	0.2
QZO-DER F15	**DOX F15**	3	4	0.3
QZO-DER F16	**DOX F16**	5	3	0.3
QZO-DER F17	**DOX F17**	1	2	0.2
Center points				
QZO-DER F4	**DOX F4**	3	3	0.2
QZO-DER F7	**DOX F7**	3	3	0.2
QZO-DER F8	**DOX F8**	3	3	0.2
QZO-DER F9	**DOX F9**	3	3	0.2
QZO-DER F12	**DOX F12**	3	3	0.2

- 10 mg drug was added in each preparation.
- 0.1% Tween 80 was added in each preparation.

Formula	QZO-DER					DOX SLNPS				
	Particle size (nm)	Entrapment efficacy (EE%)	%Release (36 hr)	Correlation coefficient (R2)	Order of reaction	Particle size (nm)	Entrapment efficacy EE%	%Release (36 hr)	Correlation coefficient (R2)	Order of reaction
F1	64.05±1.67	51.88 ± 1.86%	66.67± 1.86%	0.9888	hixson	22.39±1.25	57.86± 3.78%	52.06± 2.78%	0.9912	hixson
F2	56.9±1.89	50.76± 1.89%	100± 1.55%	0.928	Higuchi	19.89±3.32	56.62± 1.97%	78.08± 2.97%	0.928	Higuchi
F3	106.11±1.91	46.42± 1.78%	66.67± 1.55%	0.9547	Kors-peppas	37.096±2.34	51.78± 1.68%	52.06± 2.68%	0.9547	Kors-peppas
F4	145.67±2.56	71.54± 3.56%	83.33± 2.87%	0.9442	First order	50.93±1.21	79.80± 2.47%	65.07± 3.47%	0.9418	First order
F5	7.93±1.67	68.89± 1.87%	65.48± 3.66%	0.9719	Kors-peppas	22.77±1.56	76.84± 4.31%	51.13± 4.56%	0.9719	Kors-peppas
F6	14.61±3.76	76.94± 2.78%	90.48± 2.76%	0.9882	Higuchi	51.11±4.54	85.82± 4.56%	70.65± 2.47%	0.9882	Higuchi
F7	145.67±2.56	71.54± 3.56%	83.33± 2.87%	0.9442	First order	50.93 ±1.21	79.81± 2.47%	65.07± 1.45%	0.9418	First order
F8	145.67±2.29	71.54± 1.79%	83.33± 2.54%	0.9442	First order	50.93± 1.67	79.83± 1.45%	65.07± 3.78%	0.9418	First order
F9	145.67±5.02	71.54± 2.34%	83.33± 3.76%	0.9442	First order	50.93±1.4	79.84± 3.78%	65.07± 2.47%	0.9418	First order
F10	157.79±2.56	82.95± 3.56%	85.71± 2.87%	0.8651	Kors-peppas	55.16±1.21	92.52± 2.47%	66.93± 2.47%	0.8651	Kors-peppas
F11	52.73±2.56	74.78± 3.56%	100± 2.87%	0.9288	Kors-peppas	18.43±1.21	83.41± 2.47%	78.08± 2.44%	0.9288	Kors-peppas
F12	23.05±1.89	71.54± 5.03%	83.33± 1.66%	0.9442	First order	28.06±2.31	79.81± 2.44%	65.07±2.34%	0.9418	First order
F13	145.67±2.67	74.78± 4.17%	37.5± 1.09%	0.9273	Higuchi	50.93±3.03	83.41±2.34%	29.28± 3.89%	0.9273	Higuchi
F14	174.31±4.86	54.06± 3.67%	98± 2.54%	0.893	hixson	60.94±2.87	60.32± 3.89%	78.08± 1.93%	0.8918	hixson
F15	34.62±3.76	50.21± 1.8%	95.24± 3.87%	0.9296	First order	12.1 ±1	56± 2.86 %	74.37± 2.47%	0.9125	First order
F16	21.3±2.56	66.7± 3.56%	98± 2.87%	0.9069	Kors-peppas	72.45±1.21	74.42± 1.78 %	78.08± 2.78%	0.865	Kors-peppas
F17	47.43±1.95	59.7± 4.36%	99± 1.56%	0.9289	First order	16.58± 4	66.59± 1.83 %	78.08± 3.78%	0.9539	First order

- Every single value represents the average ± standard deviation (SD) (n=3)

Table (2): Particle size, Entrapment efficacy, and Release kinetics of QZO-DER and DOX SLNPs

Table (3): Composition, Particle size, EE %, release kinetics and Expected against observed values of particle size, EE% and %DR of optimized QZO-DER and DOX SLNPs

RUN					Results									
Formula		A: Wax (w/w) %	B: Phospholipon 90 G (W/W) %	C: Span (60%) (w/w) %	OFR SLNPs					OFX SLNPs				
					Particle size (nm)	Entrapment efficacy (EE%)	% Release (36 hr)	Correlation coefficient (R2)	Order of reaction	Particle size (nm)	Entrapment efficacy (EE%)	% Release (36 hr)	Correlation coefficient (R2)	Order of reaction
OFR1	OFX1	4.9	2.03	0.27	30.42±3.56	60.37± 1.63	93.97±0.587	0.9898	Higuchi	66.71±2.36	85.79±6.8	77.19±2.89	0.9361	First order
OFR2	OFX2	4	2.11	0.29	15.78±0.58	48.11± 0.588	100±0.25	0.986	Higuchi	46.049±3.65	58.13±0.58	72.47±1.48	0.9782	First order
OFR3	OFX3	3.68	2	0.3	7.86±0.98	64.21± 1.58	100±0.26	0.9401	Kors-peppas	46.034±2.98	65.61±0.89	56.78±3.25	0.974	First order
OFR4	OFX4	1	4	0.1	24.19±0.78	52± 2.51	100±0.247	0.5277	Higuchi	59.2±3.54	83.55±1.25	100.94±0.74	0.9633	Higuchi
OFR5	OFX5	2.81	2	0.3	6.47±0.258	72.11± 1.98	81.58±0.189	0.7999	Kors-peppas	21.36±1.25	62.62±3.45	59.82±2.98	0.9519	Higuchi
OFR6	OFX6	4.37	2.09	0.3	8.65±0.798	70.08±1.296	100±0.258	0.8866	hixson	45.98±2.78	58.13±1.45	56.78±3.78	0.9578	Higuchi

- 10 mg drug was added in each preparation.
- 0.1% Tween 80 was added in each preparation.
- Every single value represents the average ± standard deviation (SD) (n=3)

Formula	DOX									Formula	DER								
	Particle size			EE%			% DR				Particle size			EE%			% DR		
	Expected	Observed	%RSD	Expected	Observed	%RSD	Expected	Observed	%RSD		Expected	Observed	%RSD	Expected	Observed	%RSD	Expected	Observed	%RSD
OFX1	58.25	66.7	-14.5017	90.1897	85.79439	4.873403	81.1828	77.18955	4.918839	OFR1	26.3433	30.4247905	-15.4935	82.0376	60.369942	26.41186	88.3031	93.96974	-6.41726
OFX2	43.58	46.04943	-5.66037	91.25	58.13084	36.29497	73.7034	72.47225	1.670417	OFR2	12.9972	15.7887097	-21.4778	80.1859	48.115607	39.99493	82.327	100	-21.4668
OFX3	43.37	46.03447	-6.14798	91.4157	65.60748	28.23172	73.9306	56.78666	23.18923	OFR3	7.0854	7.86224282	-10.964	79.2131	64.208092	18.94258	80.7587	100	-23.8257
OFX4	51.65	59.2	-14.6227	82.2282	83.5514	-1.60918	89.7971	100.9406	-12.4096	OFR4	21.6877	24.198349	-11.5764	75.4352	52	31.06666	95.0856	100	-5.1684
OFX5	19.66	21.36719	-8.66866	87.0934	62.61682	28.10383	72.305	59.82524	17.25989	OFR5	6.77042	6.47576835	4.352044	74.0411	72.115607	2.600573	79.4577	81.58248	-2.6741
OFX6	49.6	45.98583	7.280657	93.1283	58.13084	37.57983	77.5316	56.78666	26.75676	OFR6	9.76448	8.65	11.41361	81.837	70.080925	14.36523	84.551	100	-18.2718

Table (4): Data of regression analysis and Analysis of variance of all dependent variables

Source	QZO-DER						DOX					
	PS (nm)		%DR		EE%		PS (nm)		%DR		EE%	
	***F* value**	***P* value**	***F* value**	***P* value**	***F* value**	***P* value**	***F* value**	***P* value**	***F* value**	***P* value**	***F* value**	***P* value**
Model	28.22	<0.0001	5.81	<0.0001	4.67	0.0001	20.84	<0.0001	5.54	<0.0001	9.26	<0.0001
A-Wax Percentage (w/w)	3.16	0.0108	12.78	0.01879	18.25	0.0069	59.2	<0.0001	4.47	0.0389	16.16	0.0069
B-Phosphatidyl Choline Percentage	12.53	0.00176	10.99	0.0016	8.65	0.0048	6.42	0.0141	11.06	0.0016	9.36	0.0034
C-span 60 %	41.4	<0.0001	8.88	0.0043	16.2691	0.00606	6.84	0.0114	14.35	0.0004	11.07	0.3053
AB	0.0915	0.7634	1.17	0.2845	6.36	0.0146	0.7164	0.4009	1.36	0.2488	2.93	0.0922
AC	1.99	0.1643	4.93	0.0305	6.42	0.0141	45.56	<0.0001	0.6077	0.4389	12.67	0.0008
BC	50.07	<0.0001	0.0486	0.8263	7.79	0.0072	10.47	0.002	0.8105	0.3718	32.32	<0.0001
A^2	11.65	0.0012	19.51	<0.0001	2.55	0.116	5.01	0.0292	10.28	0.0022	5.57	0.0218
B^2	41.9	<0.0001	1.68	0.2001	6.56	0.0132	37.53	<0.0001	3.43	0.0694	13.38	0.0006
C^2	101.58	<0.0001	3.72	0.0588	2.2	0.1432	15.29	0.0003	3.8	0.0564	3.68	0.0602
R^2	0.8193		0.9828		0.8286		0.8701		0.9709		0.8982	
Adjusted R^2	0.8903		0.9996		0.8368		0.8331		0.9858		0.8337	
Predicted R^2	0.8268		0.9675		0.8977		0.8415		0.9503		0.8645	
Adeq Precision	17.8188		18.6693		16.4483		16.861		17.604		19.7287	
C.V. %	1.26		1.24		1.01		4.69		1.68		1.32	
Lack of fit (P value)	0.3623		0.4849		0.5233		0. 303		0.5808		0.511	

Table (5): IC_{50} of selected formulations and the free drug on MCF-7, MDA-231, A549 and their corresponding resistant cells in addition

Compound	IC_{50} (μM)[a]										
	MCF-7	MCF-7 resistant	Reversal power	A549	A549 resistant	Reversal power	MDA-231	MDA-231 resistant	Reversal power	F180	HCT-116
Standard doxorubicin	1.12 ±0.04	22.42 ±0.04	--------	6.69 ±0.03	25.50 ± 0.01	---------	105 ±0.04	200.02 ±0.06	---------	>10	10.02 ± 0.05
Standard QZO-DER	10.4 ±0.04	3.91 ±0.03	---------	15.01 ±0.05	4.42 ±0.03	----------	8.2 ±0.03	2000.01 ±0.06	---------	>10	28.31 ± 0.015
Blank SLN	>10	>10	---------	>10	>10	--------	>10	>10	--------	>10	34.36 ± 0.02
OFR4	2.91 ±0.06	2.85 ±0.03	0.38157895	11.02 ±0.04	8.69±0.05	0.371308	8.24 ±0.04	10.21 ±0.04	19.703491	>10	8.01 ± 0.06
OFR6	6.12 ±0.04	1.68 ±0.04	1.36607143	14.31 ±0.03	4.64 ±0.03	0.904023	3.78 ±0.04	27.01 ±0.03	3.4146341	>10	6.32 ± 0.052
OFX1	1.12 ±0.05	2.88 ±0.05	7.77777778	4.11±0.04	8.81 ±0.04	1.7619581	4.8 ±0.05	6.22 ±0.03	1.4746544	>10	6.52 ± 0.062
OFX4	0.66 ±0.06	4.9 ±0.05	2.69387755	5.9 ±0.04	3.5 ±0.03	6.3749733	4.9 ±0.05	5.0 ±0.03	1.8666667	>10	7 ± 0.015

[a]Half-maximal inhibitory concentration (IC_{50}) values are the mean ± SD

to fibroblast cells and HCT-116.

CRedit Author Statement

Shahira F. El-Menshawe: Supervision**, Ossama M. Sayed**: Conceptualization Data curation, Writing- Original draft preparation. **Heba A. Abou Taleb**: Visualization, Investigation, Writing- Reviewing and Editing, **Mina A. Saweris**: Methodology, **Dana M. Zaher:** Methodology, **Hany A. Omar:** Supervision, Visualization, Investigation, Writing- Reviewing and Editing

Declaration of interests

☒ The authors declare that they have no known competing financial interests or personal relationships that could have appeared to influence the work reported in this paper.

☐The authors declare the following financial interests/personal relationships which may be considered as potential competing interests: